

Supplementary Information

Candle Soot: Onion-like Carbon, an Advanced Anode Material for Potassium-Ion Hybrid Capacitor

Jiangtao Chen,^{a,1} Bingjun Yang,^{a,b,1} Hongxia Li,^{a,b} Pengjun Ma,^a Junwei Lang,^a Xingbin Yan^{a,b,c,d,}*

^a Laboratory of Clean Energy Chemistry and Materials, State Key Laboratory of Solid Lubrication, Lanzhou Institute of Chemical Physics, Chinese Academy of Sciences, Lanzhou 730000, China

^b Center of Materials Science and Optoelectronics Engineering, University of Chinese Academy of Sciences, Beijing 100049, China

^c Institute of Nanomaterials Application Technology, Gansu Academy of Science, Lanzhou, 730000, China

^d Dalian National Laboratory for Clean Energy, Dalian Institute of Chemical Physics, Chinese Academy of Sciences, Dalian 116023, China

***Corresponding Author** Xingbin Yan

E-mail: xbyan@licp.cas.cn

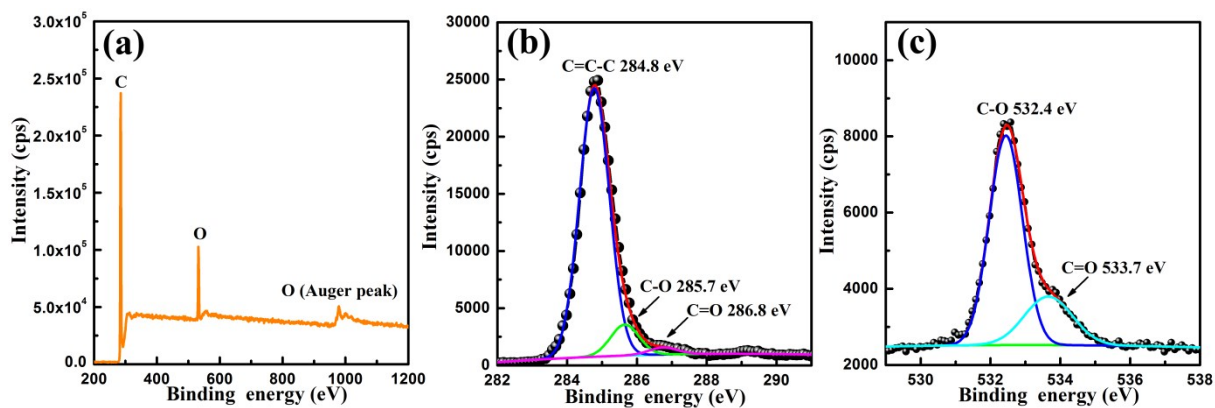


Figure S1. XPS spectra of OLC: (a) full survey, (b) C 1s and (c) O 1s.

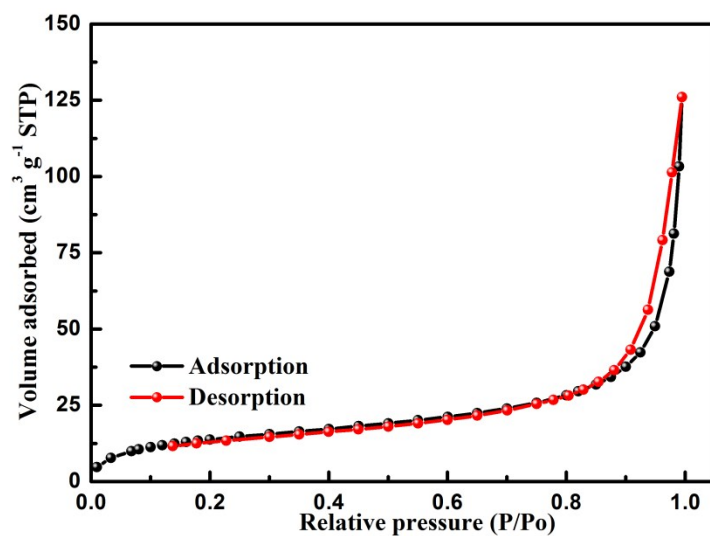


Figure S2. Nitrogen adsorption/desorption isotherm curve of OLC powders.

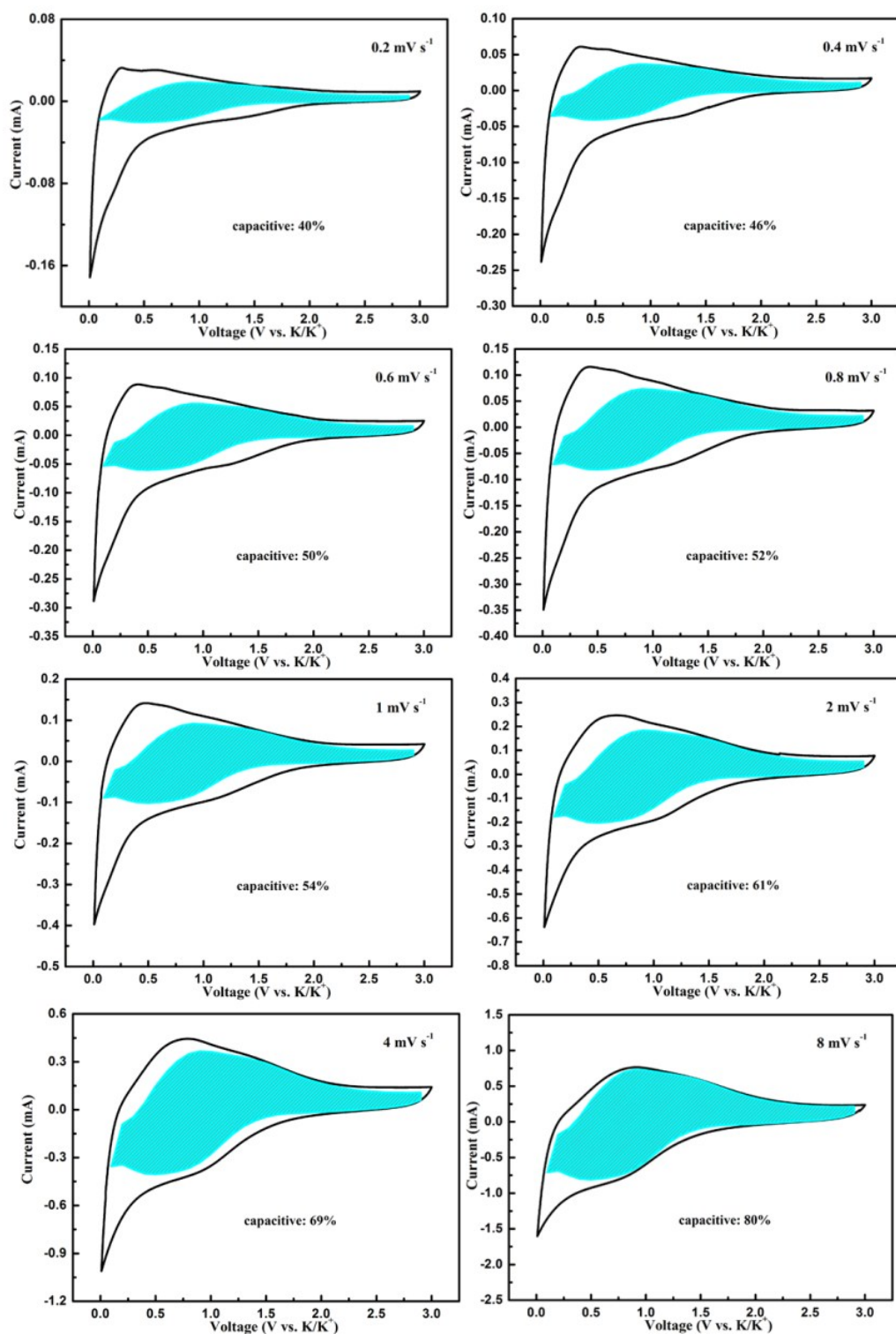


Figure S3. CV curves and related capacitive contribution areas of the OLC electrode at different scan rates. The shaded area corresponds to the capacitive current response in comparison with the total current. By calculating the area of the shadow region, the capacitive charge contributions at various sweep rates are presented in Figure 2f.

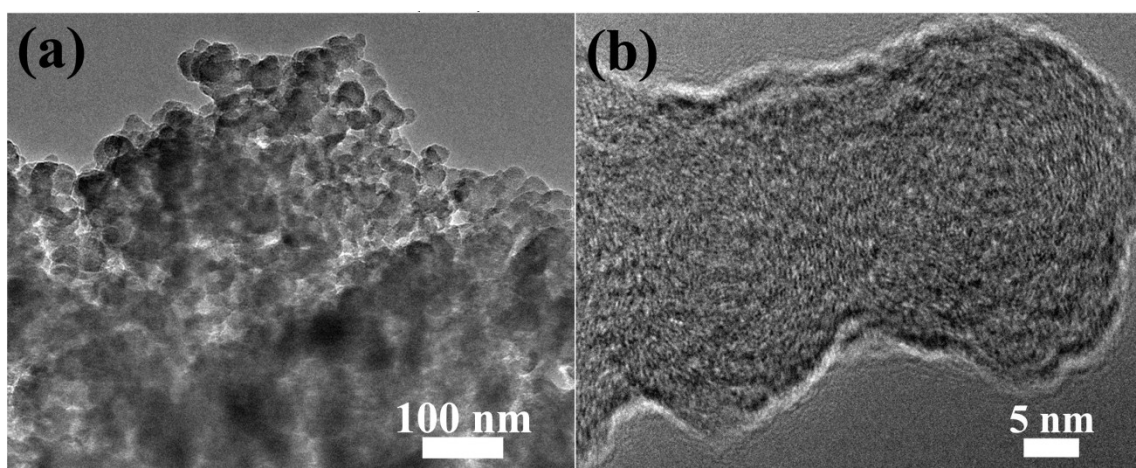


Figure S4. Low (a) and high (b) magnification TEM images of the OLC electrode under fully discharged stage (full K^+ insertion) after 1000 cycles at the rate of 2 A g^{-1} .

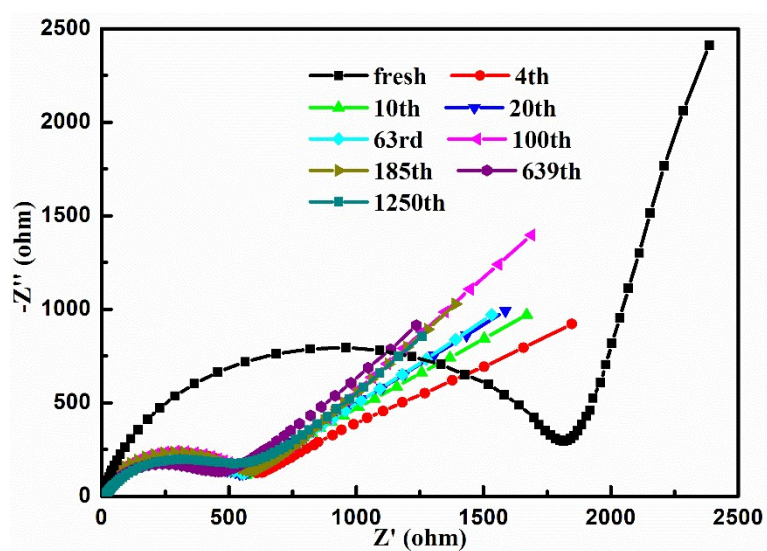


Figure S5. Electrochemical impedance spectroscopy (EIS) plots of the OLC electrode at different cycles (cycling at the current density of 1 A g^{-1}).

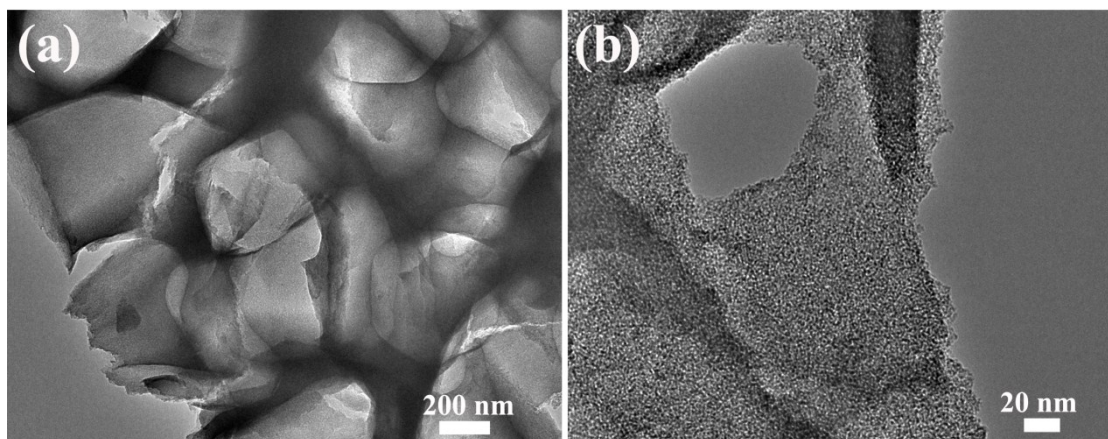


Figure S6. Low (a) and high (b) magnification TEM images of powdery AC.

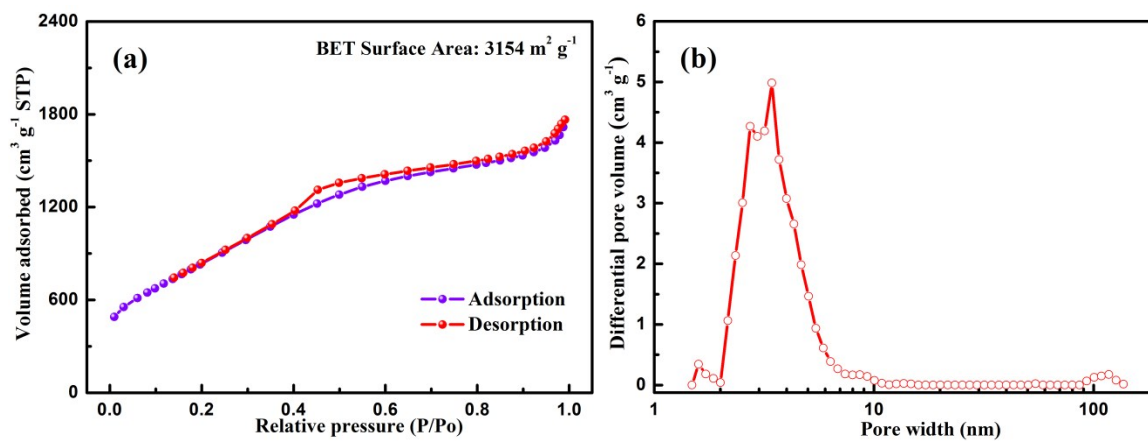


Figure S7. Nitrogen adsorption/desorption isotherm (a) and pore-size distribution (b) curves of powdery AC.

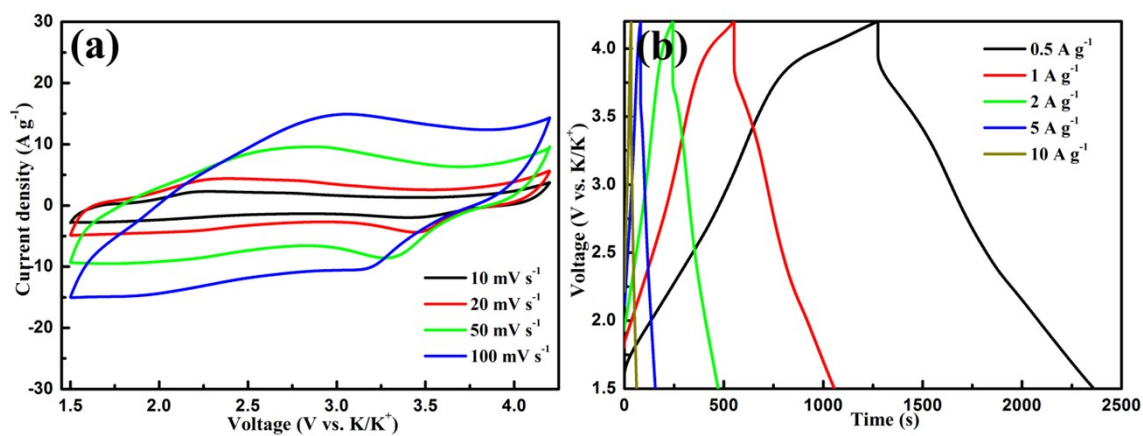


Figure S8. CV (a) and GCD (b) curves of the AC cathode at different rates.

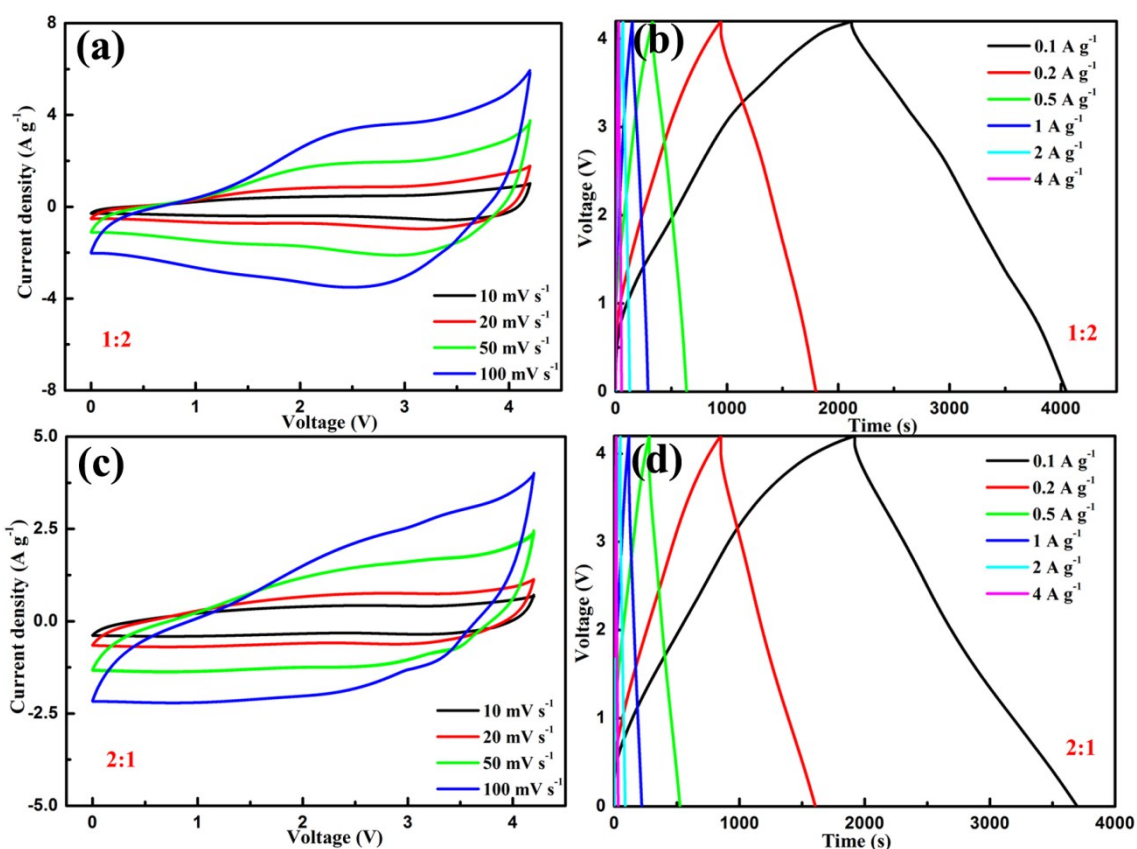


Figure S9. (a) CV and (b) GCD curves of the as-assembled PIHC device with the mass ratio 1:2 (anode to cathode). (c) CV and (d) GCD curves of the as-assembled PIHC device with the mass ratio 2:1 (anode to cathode).

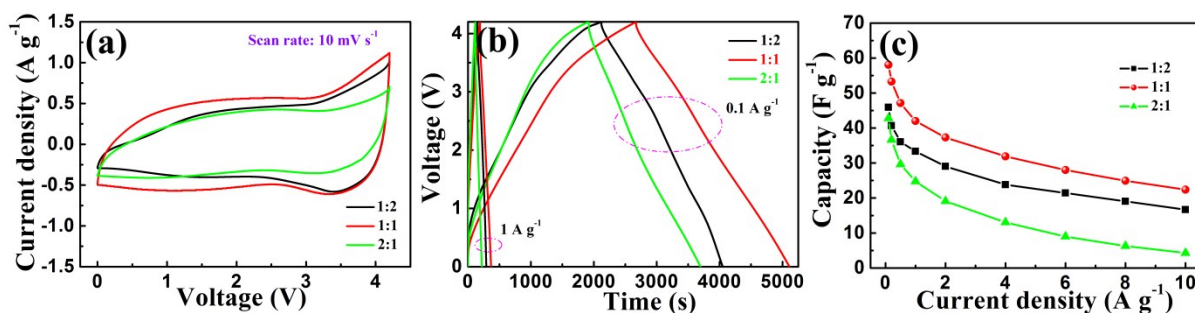


Figure S10. Comparison of the electrochemical properties of the as-assembled PIHC devices with different mass ratios of 1:2, 1:1 and 2:1 (anode to cathode). (a) CV curves at the scan rates of 10 mV s^{-1} , (b) GCD profiles at 0.1 and 1 A g^{-1} , and (c) rate performance.